

Supporting Information

Antibody responses to endemic coronaviruses modulate COVID-19 convalescent plasma functionality

William Morgenlander, Stephanie Henson, Daniel R. Monaco, Athena Chen, Kirsten Littlefield, Evan M. Bloch, Eric Fujimura, Ingo Ruczinski, Andrew R. Crowley, Harini Natarajan, Savannah E. Butler, Joshua A. Weiner, Mamie Z. Li, Tania S. Bonny, Sarah E. Benner, Ashwin Balagopal, David Sullivan, Shmuel Shoham, Thomas C. Quinn, Susan Eshleman, Arturo Casadevall, Andrew D. Redd, Oliver Laeyendecker, Margaret E. Ackerman, Andrew Pekosz, Stephen J. Elledge, Matthew Robinson, Aaron A. R. Tobian, H. Benjamin Larman

This supporting information includes:

Figures S1-S6

Tables S1 and S2

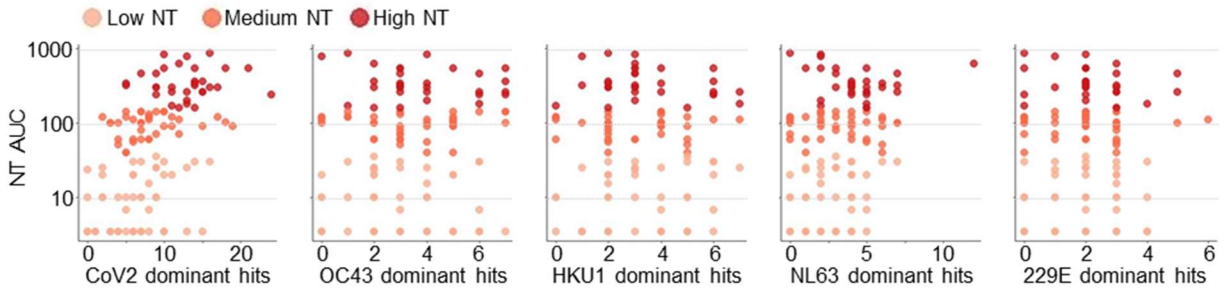


Figure S1. Polyclonality of antibody responses to CoV2 and NL63 immunodominant regions is associated with increased NT AUC

Number of reactive peptides from immunodominant regions of each coronavirus was compared to NT AUC. Polyclonal responses to CoV2 and NL63 correlate with increase NT AUC (Pearson's correlation, CoV2 $p < 10^{-8}$, $R = .49$; NL63 $p = 0.02$, $R = .21$). Low NT: $n = 55$, Medium NT: $n = 39$, and High NT: $n = 32$.

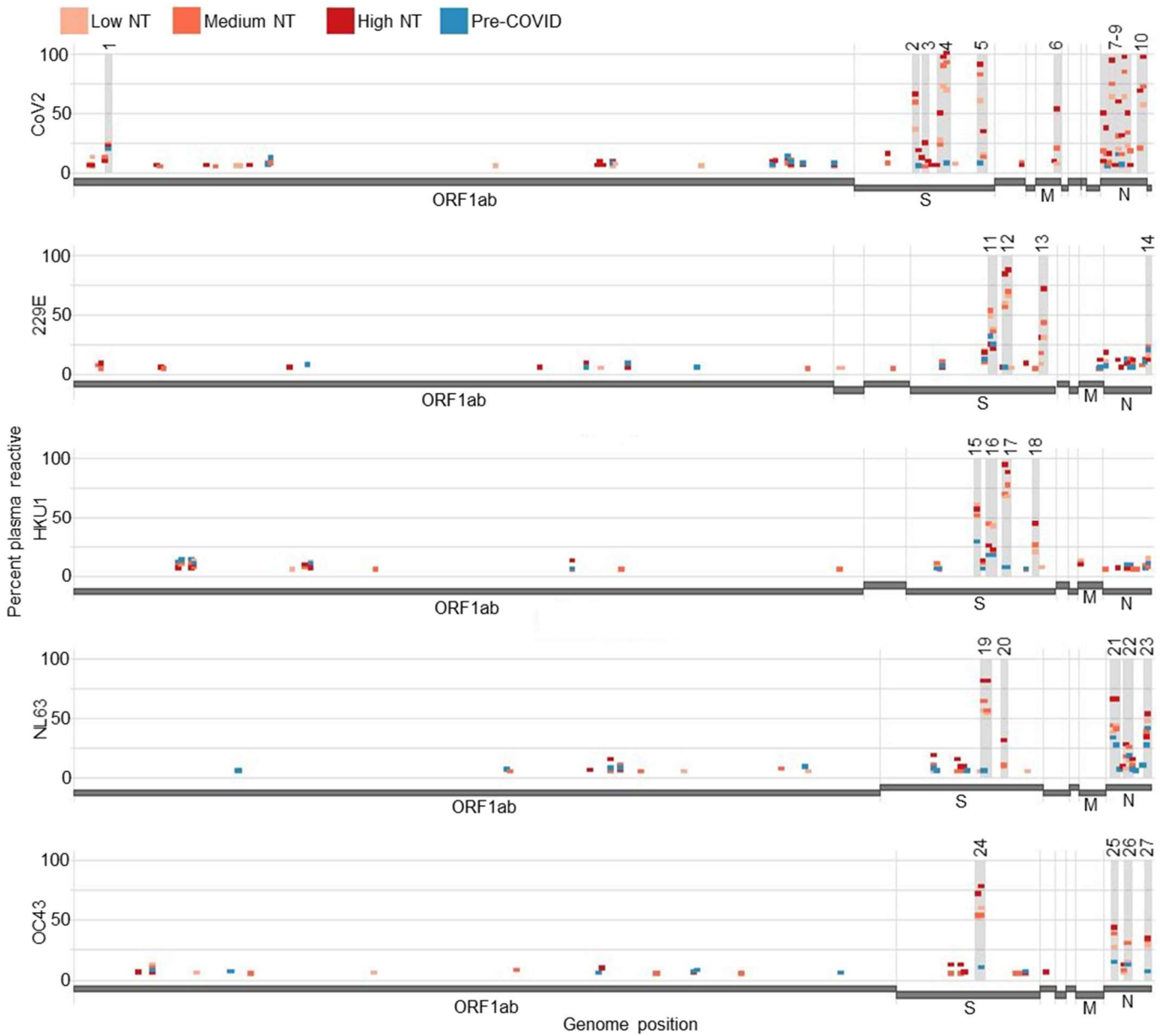


Figure S2. Whole genome reactivity plots

Antibody reactivity plots analogous to those in Figure 1 were created that include the poorly reactive ORF1. Pre-COVID: n=87, Low NT: n=55, Medium NT: n=39, and High NT: n=32.

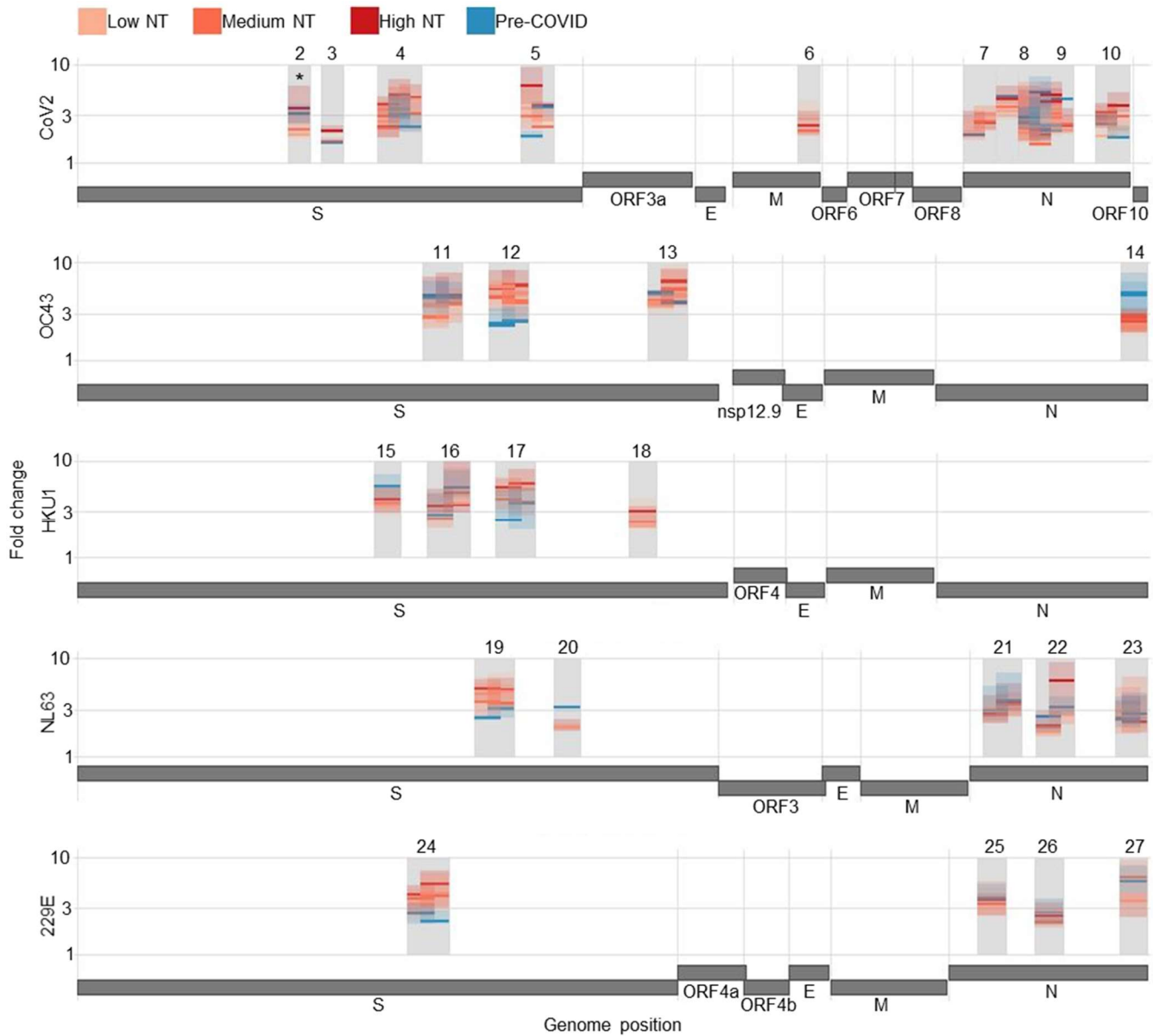
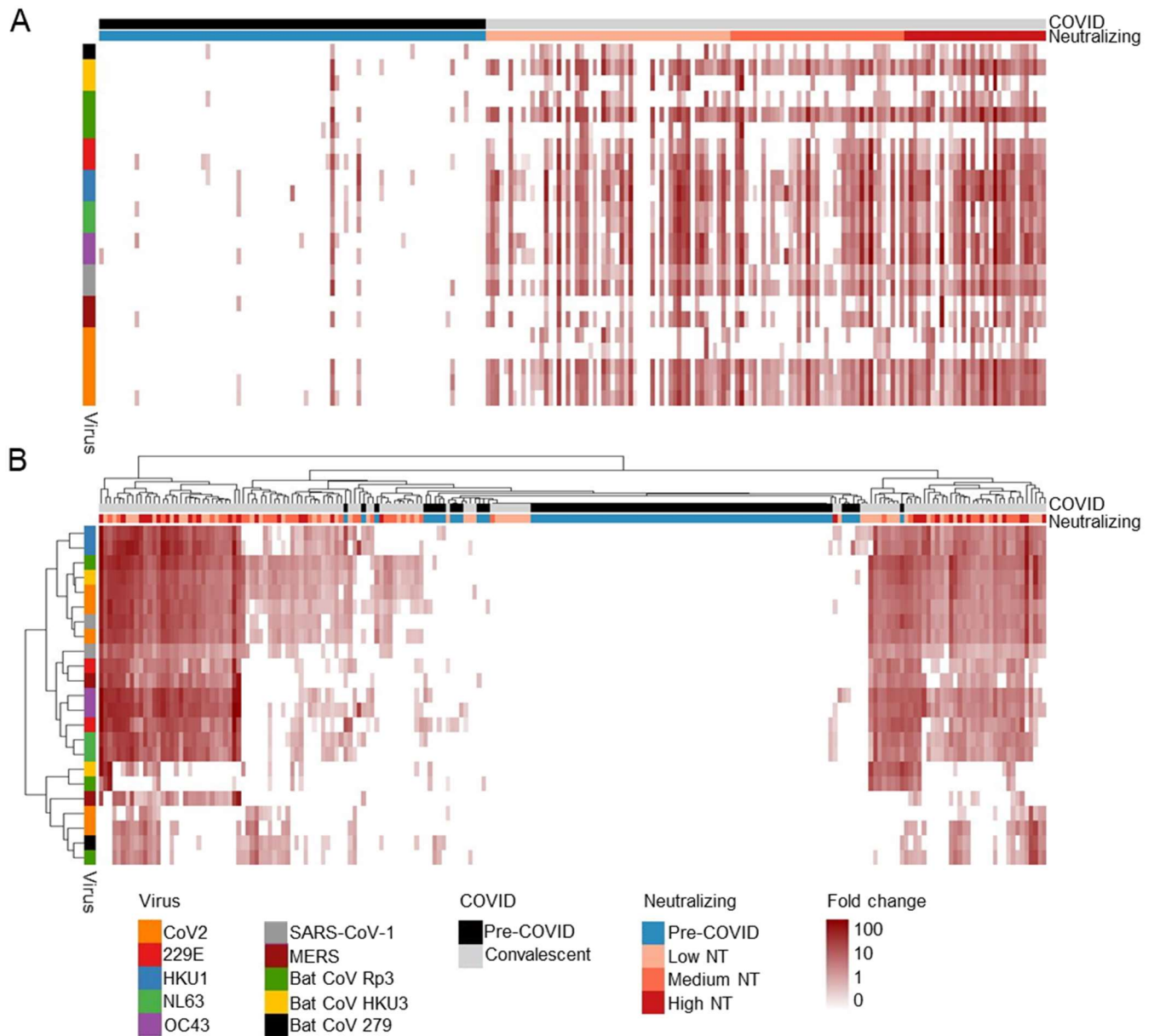


Figure S3. Magnitude of peptide reactivities does not distinguish plasma functionality

The median and interquartile range of antibody reactivity for each sample group is plotted for each immunodominant peptide. Pre-COVID: n=87, Low NT: n=55, Medium NT: n=39, and High NT: n=32. One CoV2 S immunodominant peptide (residues 533-588) indicated by asterisk show greater magnitude reactivities in High NT COVID-19 convalescent plasma compared to Medium NT or Low NT CCP (Wilcox test vs Medium NT p=0.014, vs Low NT p<0.001).

| | Virus | Segment | Domain (Spike Only) | Start | End | Amino Acid Sequence |
|----|------------|---------|---------------------|-------|------|--|
| 1 | SARS-CoV-2 | ORF1 | | 281 | 336 | IKTIQPRVEKKKLDGFMGRIRSVYPVAVSPNECNQMCLSTLMKCDHCGETSWQGTGDF |
| 2 | SARS-CoV-2 | S | RBD | 533 | 588 | LVKNKCVNFNFNGLTGTGVLTESNKKFLPFQQFGRDIADTTDAVRDPQTLEILDIT |
| 3 | SARS-CoV-2 | S | CS | 617 | 672 | CTEVPVAIHADQLTPTWRVYVSTGSNVFQTRAGCLIGAHEVNNNSYECDIPIGAGICA |
| 4 | SARS-CoV-2 | S | FP | 757 | 812 | GSFCTQLNRALTGIAVEQDKNTQEVFAQVKQIYKTPPIKDFGGFNFSQILPDPSPK |
| | | | | 757 | 812 | GSFCTQLNRALTGIAVEQDKNTQEVFAQVKQIYKTPPIKDCGGFNFSQILPDPSPK |
| | | | | 785 | 840 | VKQIYKTPPIKDCGGFNFSQILPDPSPKSKRSFIEDLLFNKVTLADAGFIKQYGDC |
| | | | | 785 | 840 | VKQIYKTPPIKDFGGFNFSQILPDPSPKSKRSFIEDLLFNKVTLADAGFIKQYGDC |
| | | | | 813 | 868 | SKRSFIEDLLFNKVTLADAGFIKQYGDCGLGDIARDLCAQKFNGLTVLPPLTDE |
| 5 | SARS-CoV-2 | S | HR2 | 1121 | 1176 | FVSGNCDVIVGNNTVYDPLQPELDSFKEELDKYFKNHTSPDVLDLGDISGINASV |
| | | | | 1149 | 1204 | KEELDKYFKNHTSPDVLDLGDISGINASVNIQKEIDRLNEVAKNLNESLIDLQLELG |
| 6 | SARS-CoV-2 | M | | 169 | 224 | ITVATSRTLSYYKLGASQRVAGDSGFAAYSRYRIGNYKLNTHSSSSDNIALLVQ* |
| 7 | SARS-CoV-2 | N | | 1 | 56 | MSDNGPQNQRNAPRITFGGSDSTGSNQNNGERSGARSKQRRPQGLPNNTASWFTAL |
| | | | | 29 | 84 | NGERSGARSKQRRPQGLPNNTASWFTALTQH GKEDLKFPRGGQVPINTNSSPDDQI |
| 8 | SARS-CoV-2 | N | | 85 | 140 | GYRRATRRIRGGDGKMKDLSRWYFYFLGTGPEAGLPYGANKDGIWVATEGALN |
| | | | | 141 | 196 | TPKDHIGTRNPANNAIVLQLPQGTTLPKGFYAEGRGGSQASSRSSSRSRNSLRN |
| | | | | 141 | 196 | TPKDHIGTRNPANNAIVLQLPQGTTLPKGFYAEGRGGSQASSRSSSRSRNSLRN |
| | | | | 169 | 224 | KGFYAEGRGGSQASSRSSSRSRNSRSTPGSSRGTSPARMAGNGGDAALALLL |
| | | | | 169 | 224 | KGFYAEGRGGSQASSRSSSRSRNSRSTPGSSRGTSPARMAGNGGDAALALLL |
| 9 | SARS-CoV-2 | N | | 197 | 252 | STPGSNRGTSPARMAGNGGDAALALLLDRLNQLESKMSGKQQQQGQTVTKKSA |
| | | | | 197 | 252 | STPGSSRGTSPARMAGNGGDAALALLLDRLNQLESKMSGKQQQQGQTVTKKSA |
| | | | | 225 | 280 | DRLNQLESKMSGKQQQQGQTVTKKSAEASKPRQKRTATKAYNVTQAFGRRGPE |
| | | | | 337 | 392 | IKLDDKDSNFKDQVILLNKHIDAYKTFPPTPKDKKKKKADEQALPQRQKQQT |
| | | | | 337 | 392 | IKLDDKDPNFKDQVILLNKHIDAYKTFPPTPKDKKKKKADEQALPQRQKQQT |
| 10 | SARS-CoV-2 | N | | 365 | 420 | PTEPKDKKKKKADEQALPQRQKQQTVLLPAADLDDFSKQLQSSMSSADSTQA* |
| | | | | 729 | 784 | NSTAISVQTCDLTVGSGYCVDYKSKNRRSRGAIITTYRFTNFEPFTVNSVNDLEPV |
| | | | | 757 | 812 | QRQRGHKNGQGENDNISVAVPKSRVQKNSRELTAEISLLKKMDEPYTEDTSEI* |
| 11 | OC43 | S | CS | 869 | 924 | PQRQRGHKNGQGENDNISVAVPKSRVQKNSRELTAEISLLKKMDEPYTEDTSEI |
| 12 | OC43 | S | FP | 897 | 952 | RGAITTYRFTNFEPFTVNSVNDLEPVGGLYEIQIPSEFTIGNMVEFIQTSSPKV |
| 13 | OC43 | S | HR2 | 1205 | 1260 | VVMSTCAVNYTKAPYVMLNLSIPNLPDFKEELDQWFKNQTSVAPDLSLDYINVT |
| | | | | 1233 | 1288 | CSKASSRSAIEDLLFDKVKLSDVGFVEAYNNCTGGAEIRDLCVQSYKGIKVLPL |
| 14 | OC43 | N | | 393 | 448 | LSTKLDKGVNFNVDINFPVLGCLGSECSKASSRSAIEDLLFDKVKLSDVGFVEA |
| | | | | 394 | 449 | FKEELDQWFKNQTSVAPDLSLDYINVTFLDLQVEMNRLQEAIKVNLQSYINLKDIG |
| 15 | HKU1 | S | RBD | 617 | 672 | GVCVNYDLYGITGGIFKEVSAAYYNNWQNLLYDSNGNIIGFKDFLTKNTYITLPC |
| 16 | HKU1 | S | CS | 729 | 784 | YSVSSCDLRMSGGFCIDYALPSSRRKRRISSPYRFVTFEPFNVSFVNDVETVGG |
| | | | | 757 | 812 | GISSPYRFVTFEPFNVSFVNDVETVGGLEIPIQNTFTIAGHEEFITSSPKVTI |
| 17 | HKU1 | S | FP | 869 | 924 | SNLNTNLHSDVDNIDFKSLLGCLGSGCQSSSRSLLEDLLFNKVKLSDVGFVEAYNN |
| | | | | 897 | 952 | SSSRSLLEDLLFNKVKLSDVGFVEAYNNCTGGSEIRDLLCVQSFNGIKVLPILSE |
| 18 | HKU1 | S | HR2 | 1149 | 1204 | KPTSFKTVLVSPGLCLSGDRGIAPKQGYFIKQNDSWMFTGSSYYPEPISDKNVVF |
| 19 | NL63 | S | FP | 841 | 896 | SLANVTSFGDYNLSSVLPQRNIHSSRIAGRSALEDLLFSKVVTSGLGTVDVDYKSC |
| 20 | NL63 | S | HR1 | 869 | 924 | GRSALEDLLFSKVVTSGLGTVDVDYKSCTKGLSIADLACAQYNGIMVLPGVADAE |
| 21 | NL63 | N | | 1009 | 1064 | IALNKIQDVVNQGSALNHLTSQLRHNFAQISNSIQAIYDRLDSIQADQQVDRLIT |
| | | | | 29 | 84 | SDKAPYRVIPIRNLVPIGKGNKDEQIGYWNVQERWRMRQRVLDLPPKVHFYFLGTG |
| 22 | NL63 | N | | 57 | 112 | NVQERWRMRQRVLDLPPKVHFYFLGTGPHKDLKFRQRSDGVVWAKEGAKTVNTS |
| | | | | 141 | 196 | EDRSNNSSRASSRSTRNNSRDSSRSTSRQQSRTRSDSNQSSDLVAAVTLALKNL |
| 23 | NL63 | N | | 169 | 224 | RQQRTRSDSNQSSDLVAAVTLALKNLGFDNQSKSPSSSGTSTPKKPNKPLSQPR |
| | | | | 309 | 364 | KMLVAKDNKLNPKFIEQISAFKPKSSIKEMQSSHAVQNTVLNASIPESKPLADD |
| 24 | 229E | S | FP | 323 | 378 | IEQISAFKPKSSIKEMQSSHAVQNTVLNASIPESKPLADDSDAIIEIVNEVLH* |
| | | | | 645 | 700 | SADVSEMLTFDKKAFTLANVSSFGDYNLSSVIPSLPTSGSRVAGRSAIEDILFSKL |
| 25 | 229E | N | | 673 | 728 | SSVIPSLPTSGSRVAGRSAIEDILFSKLVTSGLGTVDADYKCKTKGLSIADLACAQ |
| 26 | 229E | N | | 57 | 112 | YWNVQKRFRTRKGRVLDLSPKLFYFLGTGPHKDAKFRERVEGVVWVAVDGAKTEP |
| 27 | 229E | N | | 169 | 224 | NPSSDRNHNSQDDIMKAVAAALKSLGFDKPKQEKDKKSAKTGTPKPSRNQSPASSQT |
| 27 | 229E | N | | 337 | 392 | GKLEELNAFTREMQQHPLLNPSTALEFNPSQTSAPATAEPVRDEVSIEDIIDEVN* |

Table S1. Amino acid sequences of immunodominant CoV2 and HCoV peptides



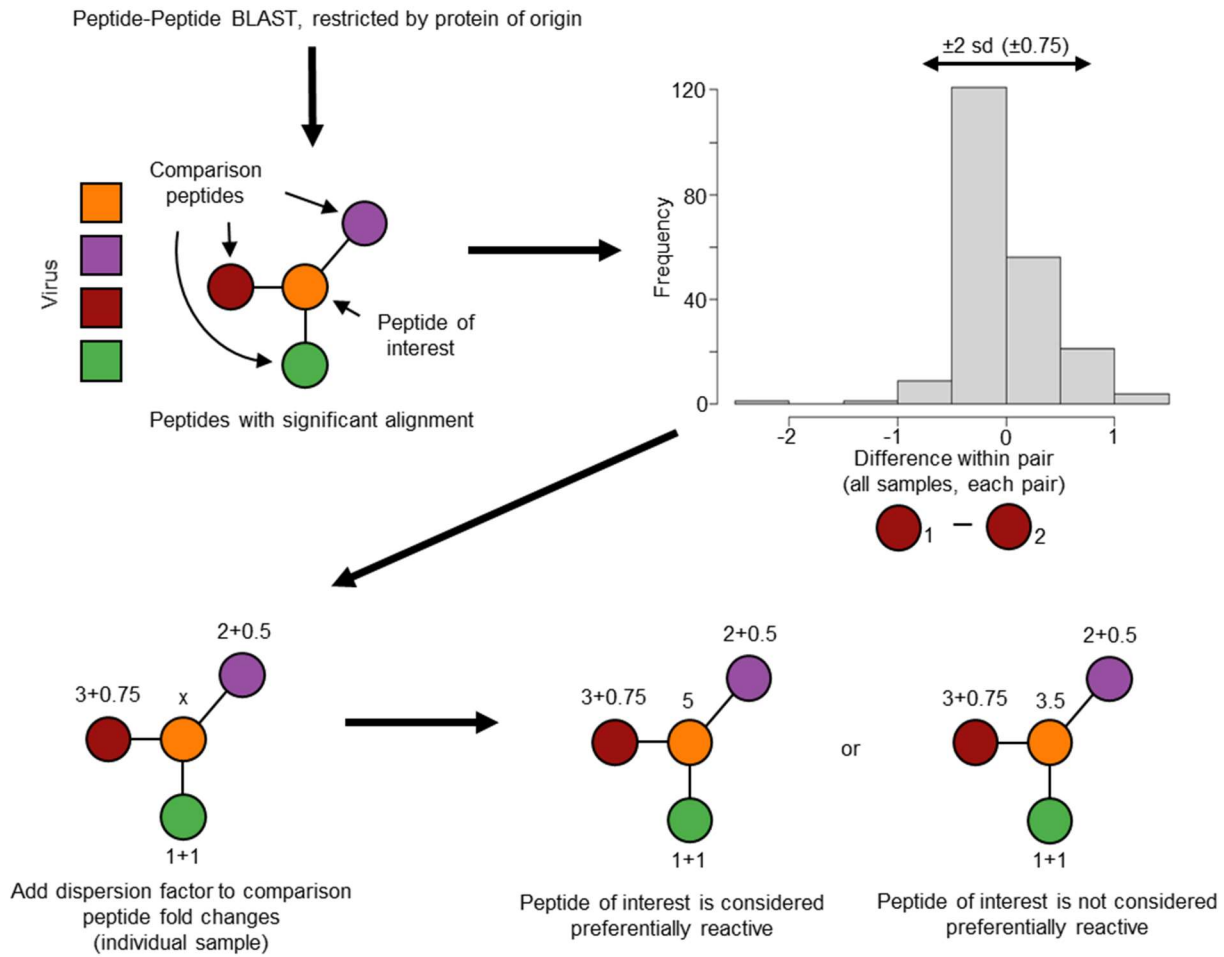


Figure S5. Deconvolution algorithm schematic

Peptides from different viruses of origin and the same protein of origin underwent peptide-peptide blast. If peptides showed significant alignment (evalue<100), they were considered potentially cross-reactive. By taking advantage of the duplicate representation of each peptide in the library, a measure of expected technical dispersion was calculated. If a target peptide displayed enrichment greater than any comparison peptide plus the factor for technical dispersion (2 standard deviations), it was considered a target-preferred reactivity.

| | Virus | Segment | Domain (Spike Only) | Start | End | Percent Samples Enriched | | | | Association with Phenotype (-log(p)) | | | |
|----|------------|---------|---------------------|-------|------|--------------------------|-------------|----------------|--------------|--------------------------------------|------|------|------|
| | | | | | | Pre-COVID n=87 | Low NT n=55 | Medium NT n=39 | High NT n=32 | NT AUC | ADCP | ADCC | ADCD |
| 1 | SARS-CoV-2 | ORF1 | | 281 | 336 | 8 | 7.3 | 10.3 | 9.4 | 0.3 | 0.2 | 0.3 | 0.2 |
| 2 | SARS-CoV-2 | S | RBD | 533 | 588 | 1.1 | 1.8 | 10.3 | 18.8 | 2.6 | 4.4 | 4.7 | 3.7 |
| 3 | SARS-CoV-2 | S | CS | 617 | 672 | 1.1 | 0 | 5.1 | 25 | 3.5 | 4.5 | 3.6 | 1 |
| 4 | SARS-CoV-2 | S | FP | 757 | 812 | 0 | 9.1 | 7.7 | 9.4 | 0 | 0.3 | 0.4 | 0.2 |
| | | | | 757 | 812 | 0 | 20 | 17.9 | 34.4 | 1 | 2.4 | 2.3 | 3.1 |
| | | | | 785 | 840 | 1.1 | 0 | 2.6 | 6.3 | 1 | 0.7 | 1 | 1.2 |
| | | | | 785 | 840 | 0 | 1.8 | 10.3 | 9.4 | 1.4 | 1.4 | 0.7 | 1.6 |
| | | | | 813 | 868 | 0 | 0 | 5.1 | 3.1 | 0.6 | 1.1 | 0.5 | 0.1 |
| 5 | SARS-CoV-2 | S | HR2 | 1121 | 1176 | 0 | 20 | 23.1 | 40.6 | 1.4 | 2.7 | 1 | 1.8 |
| | | | | 1149 | 1204 | 1.1 | 5.5 | 0 | 0 | 1.1 | 0.5 | 0.2 | 0.2 |
| 6 | SARS-CoV-2 | M | | 169 | 224 | 0 | 7.3 | 20.5 | 50 | 4.7 | 5.8 | 6.7 | 1.5 |
| 7 | SARS-CoV-2 | N | | 1 | 56 | 1.1 | 9.1 | 17.9 | 50 | 4.8 | 4.7 | 6.4 | 3.5 |
| | | | | 29 | 84 | 0 | 5.5 | 15.4 | 37.5 | 4.4 | 3.5 | 4.4 | 2.1 |
| 8 | SARS-CoV-2 | N | | 85 | 140 | 0 | 34.5 | 48.7 | 46.9 | 1.5 | 4.7 | 1.6 | 0.6 |
| | | | | 141 | 196 | 11.5 | 18.2 | 25.6 | 43.8 | 1.5 | 1 | 3.2 | 3.4 |
| | | | | 141 | 196 | 14.9 | 20 | 30.8 | 59.4 | 2.5 | 1.9 | 3.2 | 3.3 |
| | | | | 169 | 224 | 2.3 | 5.5 | 2.6 | 12.5 | 0.7 | 0.1 | 1.4 | 1 |
| | | | | 169 | 224 | 5.7 | 3.6 | 5.1 | 18.8 | 1.5 | 1 | 1.3 | 2 |
| | | | | 197 | 252 | 2.3 | 49.1 | 76.9 | 96.9 | 4.9 | 3.9 | 3.4 | 2.7 |
| | | | | 197 | 252 | 3.4 | 47.3 | 64.1 | 93.8 | 7.1 | 6.8 | 3.7 | 2.4 |
| | | | | 225 | 280 | 1.1 | 20 | 33.3 | 40.6 | 1.7 | 3 | 4.2 | 1.8 |
| 10 | SARS-CoV-2 | N | | 337 | 392 | 2.3 | 20 | 17.9 | 65.6 | 4.3 | 4.1 | 5.4 | 3.2 |
| | | | | 337 | 392 | 2.3 | 16.4 | 17.9 | 56.3 | 4.6 | 5 | 5.9 | 3.1 |
| | | | | 365 | 420 | 3.4 | 56.4 | 71.8 | 96.9 | 4.3 | 4.3 | 4.1 | 0.7 |
| 11 | OC43 | S | CS | 729 | 784 | 14.9 | 7.3 | 7.7 | 9.4 | 0 | 0.1 | 0.3 | 0.2 |
| | | | | 757 | 812 | 12.6 | 5.5 | 5.1 | 6.3 | 0.1 | 0.3 | 0 | 0.6 |
| 12 | OC43 | S | FP | 869 | 924 | 0 | 0 | 0 | 6.3 | 1.3 | 0.5 | 0.3 | 0.5 |
| | | | | 897 | 952 | 0 | 0 | 2.6 | 6.3 | 1.4 | 1.1 | 0.9 | 1 |
| 13 | OC43 | S | HR2 | 1205 | 1260 | 1.1 | 0 | 0 | 0 | 0 | 0 | 0 | 0 |
| | | | | 1233 | 1288 | 1.1 | 9.1 | 10.3 | 6.3 | 0 | 0 | 0.3 | 0.5 |
| 14 | OC43 | N | | 393 | 448 | 20.7 | 9.1 | 15.4 | 9.4 | 0.2 | 0 | 0 | 0.4 |
| | | | | 394 | 449 | 19.5 | 10.9 | 17.9 | 9.4 | 0.2 | 0 | 0.2 | 0.1 |
| 15 | HKU1 | S | RBD | 617 | 672 | 28.7 | 50.9 | 35.9 | 40.6 | 1 | 1 | 0.6 | 0.1 |
| 16 | HKU1 | S | CS | 729 | 784 | 1.1 | 7.3 | 2.6 | 6.3 | 0.1 | 0 | 0 | 0 |
| | | | | 757 | 812 | 8 | 10.9 | 2.6 | 6.3 | 0.7 | 0.2 | 0.3 | 0.1 |
| 17 | HKU1 | S | FP | 869 | 924 | 1.1 | 3.6 | 0 | 6.3 | 0.2 | 0.3 | 0.3 | 0.2 |
| | | | | 897 | 952 | 0 | 12.7 | 2.6 | 12.5 | 0 | 0.5 | 1.3 | 0.6 |
| 18 | HKU1 | S | HR2 | 1149 | 1204 | 0 | 20 | 23.1 | 43.8 | 1.6 | 2.4 | 3.1 | 4.5 |
| 19 | NL63 | S | FP | 841 | 896 | 0 | 0 | 0 | 3.1 | 0.7 | 0.9 | 0.8 | 0.6 |
| | | | | 869 | 924 | 0 | 0 | 0 | 0 | 0 | 0 | 0 | 0 |
| 20 | NL63 | S | HR1 | 1009 | 1064 | 0 | 5.5 | 5.1 | 18.8 | 1.3 | 0.3 | 0.3 | 0.3 |
| 21 | NL63 | N | | 29 | 84 | 13.8 | 5.5 | 2.6 | 0 | 1.3 | 1.2 | 0 | 0.6 |
| | | | | 57 | 112 | 16.1 | 7.3 | 12.8 | 9.4 | 0.1 | 0.6 | 0.3 | 0.8 |
| 22 | NL63 | N | | 141 | 196 | 1.1 | 3.6 | 2.6 | 12.5 | 0.8 | 0.3 | 1.1 | 0.8 |
| | | | | 169 | 224 | 17.2 | 9.1 | 15.4 | 15.6 | 0.7 | 0.1 | 0.1 | 0.2 |
| 23 | NL63 | N | | 309 | 364 | 8 | 3.6 | 7.7 | 3.1 | 0.2 | 0.2 | 0.1 | 0 |
| | | | | 323 | 378 | 14.9 | 9.1 | 15.4 | 12.5 | 0 | 0.2 | 0.1 | 0.4 |
| 24 | 229E | S | FP | 645 | 700 | 0 | 0 | 0 | 0 | 0 | 0 | 0 | 0 |
| | | | | 673 | 728 | 0 | 1.8 | 0 | 0 | 0.2 | 0.2 | 1 | 0.5 |
| 25 | 229E | N | | 57 | 112 | 5.7 | 10.9 | 5.1 | 0 | 1.8 | 1.1 | 1.2 | 0.5 |
| 26 | 229E | N | | 169 | 224 | 5.7 | 5.5 | 5.1 | 0 | 0.5 | 0.3 | 0.5 | 0.3 |
| 27 | 229E | N | | 337 | 392 | 4.6 | 10.9 | 15.4 | 9.4 | 0.4 | 0.1 | 0.2 | 0.4 |

Table S2. Deconvoluted immunodominant coronavirus peptides and their functional correlates

The frequency of enrichment of 52 immunodominant peptides among each sample group is shown post deconvolution. The percentage of samples with a specific reactivity is shown (red shading). Associations with COVID-19 convalescent plasma functionality were defined by dichotomizing all convalescent plasma by presence or absence of each particular reactivity followed by a two sided Wilcox test. The negative log transformed p values are shown (green shading).

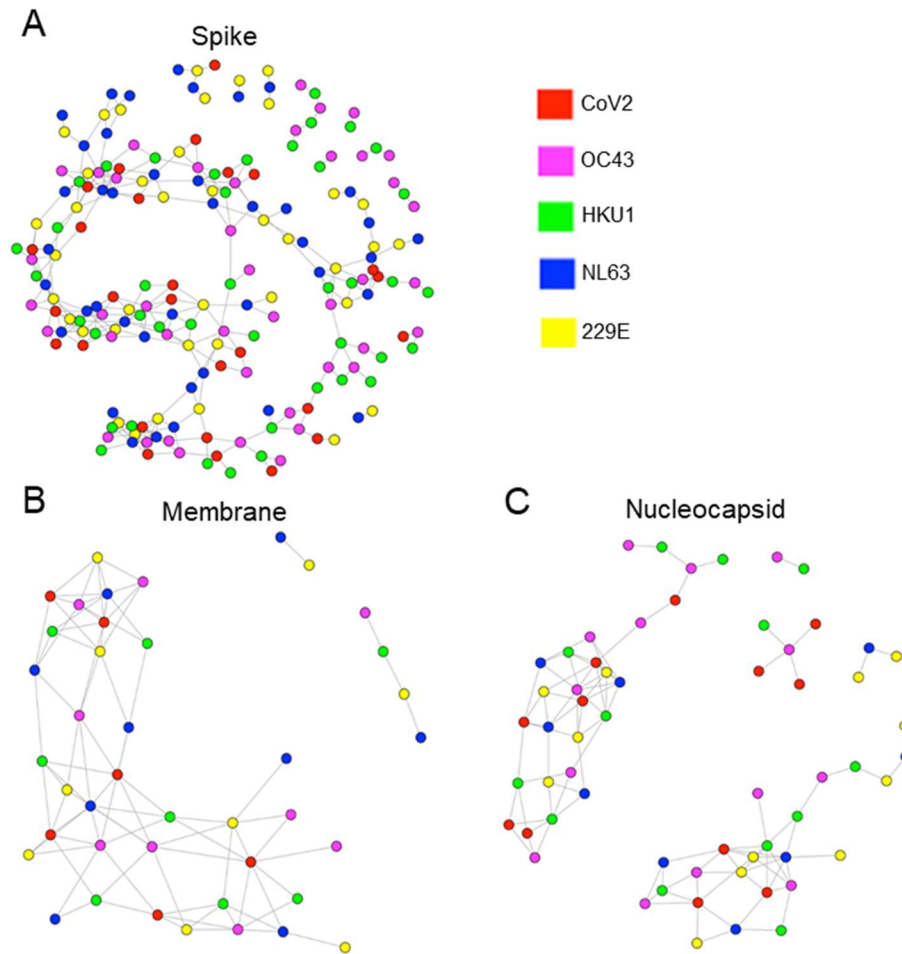


Figure S6. Visualization of CoV2 and HCoV peptide sequence homologies

Network graphs show sequence homologies among the spike (A), membrane (B) and nucleocapsid (C) peptides between CoV2 and each HCoV. Nodes (peptides) are colored by their corresponding virus. Peptides are linked by an edge if they share blastp sequence similarity. Only homologies among peptides from different viruses are shown for simplicity.